Available online at www.sciencedirect.com
SCIENCE DIRECT
Journal of Catalysis 238 (2006) 309–320
JOURNAL OF CATALYSIS
www.elsevier.com/locate/jcat

Low-temperature steam reforming of jet fuel in the absence and presence of sulfur over Rh and Rh–Ni catalysts for fuel cells

James J. Strohm, Jian Zheng, Chunshan Song *

Clean Fuels and Catalysis Program, The Energy Institute, and Department of Energy & Geo-Environmental Engineering, The Pennsylvania State University, 209 Academic Projects Building, University Park, PA 16802, USA

Received 5 September 2005; revised 28 November 2005; accepted 5 December 2005

Available online 20 January 2006

Abstract

This work is a comparative study on low-temperature steam reforming of jet fuel over Rh and Rh–Ni loaded on CeO_2-modified Al_2O_3 support in the absence and presence of different amounts of organic sulfur. Rh loaded on CeO_2–Al_2O_3 support can promote reforming of sulfur-free or desulfurized jet fuel at <520 °C with >97% conversion to syngas and CH_4. However, monometallic Rh/CeO_2–Al_2O_3 catalyst deactivates by S poisoning. During the reforming of liquid fuel with >10 ppmw S, catalytic activity rapidly decreases when the amount of sulfur in the fuel flown over the catalyst reaches the level corresponding to a S_{fuel}:Rh_{surf} atomic ratio of 0.28–0.30 (for which the amount of surface Rh is based on H_2 and CO pulse chemisorption analysis). Methane formation is even more sensitive (than conversion) to sulfur poisoning. At a S_{fuel}:Rh_{surf} ratio of 0.15, methane selectivity over the Rh/CeO_2–Al_2O_3 catalyst begins to decline. Addition of Ni by co-impregnation into the Rh/CeO_2–Al_2O_3 catalyst leads to much higher sulfur tolerance. Ni acts as a protective and sacrificial metal for Rh in the Rh–Ni/CeO_2–Al_2O_3 catalyst. Ni surface saturation of sulfur was found to occur at a S_{fuel}:Ni_{surf} ratio of 0.59–0.60, corresponding to a S_{fuel}:Rh_{surf} ratio of 1.1 for 2% Rh–10% Ni/CeO_2–Al_2O_3. The bimetallic Rh–Ni/CeO_2–Al_2O_3 catalyst allows for successful low-temperature reforming of a JP-8 jet fuel containing 22 ppm sulfur for 72 h with >95% conversion. TPR and XPS analysis reveals close Rh–Ni metal–metal interactions. The presence of Ni increases the temperature for Rh reduction in TPR, whereas Rh helps maintain Ni in a reduced state in an oxidative atmosphere.

Keywords: Catalyst; Rh; Rh–Ni; Bimetallic; Steam reforming; Jet fuel; Sulfur tolerance

1. Introduction

Fuel processing has become an important subject in catalysis research for fuel cells [1–4]. The demand for on-site and on-board syngas and hydrogen production is increasing with growing interest in hydrogen energy and fuel cells for the supply of cleaner and more efficient electric power supply [1–4]. Steam reforming of logistic fuels, such as jet fuel and diesel fuel, is a viable and effective means of syngas and hydrogen production for solid-oxide fuel cell and proton-exchange membrane fuel cell, respectively, due to the existing infrastructure and high energy density of these fuels. Along with the advantages of using liquid hydrocarbons for portable and stationary fuel processors are some major challenges, as discussed in a recent review [3].

Industrial hydrogen production is generally conducted by steam reforming of natural gas over supported nickel catalysts [5–7]. Numerous studies have been conducted on strategies for processing conditions and catalyst formulations to minimize carbon formation during steam reforming [8–12]. However, the use of higher hydrocarbons that contain aromatics can pose a threat of carbon formation during steam reforming both on the catalyst and before the catalyst bed [13]. One approach to minimizing carbon formation on the catalyst is by using noble metals, such as Ru and Rh, which do not produce carbon filaments due to poor carbon solubility in the metal [13]. Another approach is to first perform low-temperature steam reforming (or prereforming) to reform the higher hydrocarbons to methane, hydrogen, and carbon oxides, followed by high-temperature reforming of the reformate into hydrogen and carbon oxides.

* Corresponding author. Fax: +1 814 865 3248.
E-mail address: csong@psu.edu (C. Song).

0021-9517/$ – see front matter
doi:10.1016/j.jcat.2005.12.010

Prereforming of liquid hydrocarbons can significantly reduce the risk of carbon formation from pyrolysis of the fuel before it reaches the catalyst bed. Then the reformate can be heated to reforming temperatures above 700 °C with minimal risk of carbon formation [13,14]. This high-temperature reforming step can be done either inside the solid oxide fuel cell stack or in a separate reformer system.

Another major challenge in the reforming of logistic fuels is the inherent sulfur content, which can range from about 300–3000 ppm or higher. Sulfur can be removed via deep desulfurization using novel hydrotreating catalysts or by deep adsorptive desulfurization [15–27]. Sulfur-free fuels, such as Fischer–Tropsch diesel, currently are not widely available; hence on-board or on-site desulfurization and sulfur-tolerant reforming catalysts are necessary [3]. Much work has been done to better understand the sulfur poisoning of Ni-based reforming catalysts [14,28–31] and Rh-based catalysts [32–34]; however, a highly active sulfur-tolerant steam-reforming catalyst has not yet been developed.

The objectives of this work are to study the catalytic effectiveness and deactivation behavior of Rh-based catalysts for low-temperature steam reforming of liquid fuels using model and real jet fuel as the feedstock in the absence and presence of organic sulfur, and also to explore ways to improve the sulfur tolerance of Rh-based catalysts by investigating the role of Ni addition toward developing a highly active and sulfur-tolerant catalyst for the steam reforming of logistic fuels. The impact and role of Ni as a modifier to retard the sulfur poisoning of Rh are examined.

2. Experimental

2.1. Catalysts

γ-Al_2O_3 (UOP LaRoche VGL-15) was used for preparing 20 wt% CeO_2–Al_2O_3 (Ce–Al) by wet impregnation of $Ce(NO_3)_2$ followed by calcination at 550 °C. For the Rh loading, $Rh(NO_3)_3$ was wet-impregnated onto the prepared Ce–Al support. Our preliminary work indicated that the Rh catalyst derived from $Rh(NO_3)_3$ was better than that derived from $RhCl_3$ in terms of better metal dispersion and improved catalyst activity for reforming. The impregnated catalyst was then dried at 100 °C overnight, followed by calcination at 550 °C, for a nominal Rh loading of 2 wt% for all catalysts studied. For the Rh–Ni bimetallic catalysts, unless described otherwise, the Ni and Rh were co-loaded via wet co-impregnation using a solution of the respective metal nitrates, then dried overnight at 100 °C, followed by calcination at 550 °C. Several control catalysts were prepared with a different support (the γ-Al_2O_3 without CeO_2) using the same impregnation procedure.

2.2. Fuel formulations

A model jet fuel (MJF) comprising 10 mol% trimethylbenzene, 5 mol% ethylbenzene, and 5 mol% *n*-butylbenzene in dodecane was used to simulate a sulfur-free jet fuel. Sulfur-tolerance experiments were conducted using NORPAR-13, an industrial solvent from Exxon Mobil comprising only normal paraffins with an average carbon number of 13 containing 4 ppm sulfur, which simulates a paraffinic jet fuel because dodecane and tetradecane are known major components of jet fuels [35,36]. The NORPAR-13 was doped with 3-methylbenzothiophene to yield sulfur concentrations of 15, 35, and 100 ppm. 3-Methylbenzothiophene is a major component of the sulfur compounds in jet fuels [37]. For convenience, in the remainder of this paper we refer to the NORPAR-13 as 4 ppm NORPAR-13, 35 ppm NORPAR-13, and so on, with *x* ppm denoting the sulfur content of the model fuel.

A jet fuel, JP-8, was fractionated to 70% of the initial volume with a rough cut of 220 °C, followed by sulfur reduction via an adsorptive desulfurization process developed at The Pennsylvania State University [17,19,22,23]. The final treated JP-8 contains 22 ppm of sulfur as analyzed by an Antex 900ES total sulfur analyzer.

2.3. Reaction conditions

Approximately 1.0 g of catalyst with particle sizes of 18–35 mesh (0.5–1 mm) was placed in the center of a stainless steel reactor tube (0.54 inch o.d., 0.375 inch i.d., 24 inches long), and the rest of the tube was packed with α-alumina beads. Catalyst reduction was performed in situ at 500 °C (at a heating rate of 2 °C/min) under a 20-mL/min hydrogen flow (UHP grade) for 5 h. A preheater was designed to minimize carbon formation at the low flow rates used.

To start the experiment, steam was introduced into the reactor for 30 min before the fuel was introduced. Both the water and fuel were pumped via HPLC pumps through the preheater and then into the reactor at volumetric flow rates of 4.08 and 1.38 mL/h, respectively, for a steam-to-carbon molar ratio of 3:1. After the first 30 min of fuel introduction, the nitrogen flow was reduced from 35 to 1 mL/min and used as an internal standard for gas chromatography (GC) quantification. The WHSV ($g_{reactants}/(h\,g_{cat})$) of the experiments was 5.13 h^{-1} (feed GHSV of ∼2785 h^{-1}, assuming ideal gas at reaction temperature of 515 °C with 0% conversion). The experiment was terminated by increasing the nitrogen flow to 120 mL/min and switching off the fuel and steam valves. The furnace was then opened and cooled to below 100 °C within 60 min.

2.4. Analysis

For product selectivity, an on-line SRI multigas analyzer gas chromatograph equipped with a thermal conductivity detector was used for the analysis of H_2, CH_4, CO, and CO_2 products (and other light hydrocarbons, when present). During the experiment, the liquid products were collected in a liquid condenser, and volume measurements were taken for calculation of the total conversion. The assumption that all of the remaining fuel in the liquid products is of the same composition as the initial fuel was confirmed using GC-mass spectroscopy (MS) analysis for catalyst activity above ∼75%. Error analysis for conversion measurements was performed by mixing known amounts of fuel and water corresponding to various conversion levels,

which yielded an average error of ±0.3% conversion for a 2-h sampling period at a conversion of 98%.

Temperature-programmed oxidation (TPO) was used to determine the total amount of carbon species formed and/or adsorbed on the catalyst. TPO analysis was conducted using a LECO RC-412 multiphase carbon determiner with UHP-grade oxygen passed over the sample as it was heated from 100 to 900 °C at a rate of 30 °C/min.

Temperature-programmed reduction (TPR) was conducted using freshly calcined catalyst samples on a Micrometrics TPR/TPD AutoChem 2910 with 5% hydrogen in argon with a temperature ramp of 5 °C/min. Carbon monoxide and hydrogen pulse chemisorption was conducted using this same device. Sample preparation involved reducing the sample in hydrogen to 280 °C at a rate of 5 °C/min, followed by cooling to 50 °C under inert gas, then pulsing with 24.3% H_2 in argon or 10.5% CO in helium. By first heating to only 280 °C in hydrogen, only the RhO_x should be reduced, with minimal reduction of NiO. Immediately after pulsing, the sample was then reheated in the presence of hydrogen to 500 °C, to reduce NiO species on the catalyst. The sample was then cooled under inert gas to 50 °C and pulsed with the appropriate gas.

Control experiments for pulse chemisorption on just Rh–CeAl and Ni–CeAl were also performed. With reduction at only 280 °C, no detectable hydrogen uptake was observed for the Ni–CeAl catalyst. When the Rh catalyst was reduced at 500 °C, the amount of hydrogen uptake was within experimental error of the hydrogen uptake when reduced to 280 °C. Evidence from TPR profiles and the control pulse chemisorption experiments suggests that only RhO_x is reduced when heated in H_2 at 280 °C, and subsequent pulses are an indication of the Rh surface area. The difference in the volumetric hydrogen uptake at 500 and 280 °C is an indication of the H adsorption only on Ni, which can then be used for Ni dispersion calculations.

XPS analysis was performed on a Kratos Analytical Axis Ultra using an X-ray source of monochromatic alumina (1486.6 eV) at 280 W, with pass energies of 80 eV (survey) and 20 eV (high-resolution) with step sizes of 0.5 and 0.1 eV, respectively. The catalyst powders were pressed into 5 × 5 mm 3M double-sided tape using a mortar and pestle and visualized by a stereomicroscope to ensure complete and uniform coverage. For the reduced catalyst samples, reduction was performed ex situ as described for pulse chemisorption experiments. After reduction, all samples were immediately stored in a continuous purge stream of nitrogen within a glove box. Sample preparation was performed as described above, and the samples were then exposed to air at room temperature for 24 h.

Sample height positions were set from a O 1s signal at 529 eV after changing the lateral coordinates such that the measured signals from the sample powders were maximized, thus minimizing any possible signal from the 3M double-sided tape. The 3M double-sided tape was measured independently, and the characteristic shape of the C 1s line was not found when compared with the C 1s line collected during sampling. XPS quantification was performed by applying the appropriate relative sensitivity factors (RSFs) and spectrometer transmission function for the Kratos instrument to the integrated peak areas. These RSFs take into consideration the X-ray cross-section and average attenuation length and instrumental factors related to X-ray source position, sample position, and spectrometer position. The spectrometer transmission function was corrected to a NPL calibration standard for the particular pass energy, magnification lens, aperture and iris settings, and transmission function of the spectrometer. The average sampling depth set on the C 1s line from an alumina powder was 30 Å.

A survey scan was initially recorded for the sample to identify the elements present. Composition as well as chemical states were determined from the charge-corrected high-resolution scans. All binding energies were referenced to Al 2p at 74.7 eV.

3. Results and discussion

3.1. Basic characterization of catalysts

Table 1 gives the results of basic characterization of the Rh and Rh–Ni catalysts prepared and examined in this work. For comparison, the table also lists some Ni catalysts prepared on the same support without Rh. Coating the Al_2O_3 support with CeO_2 decreased the surface area, so that the catalysts supported on CeO_2–Al_2O_3 tended to have somewhat lower surface area than those supported on Al_2O_3. Both H_2 and CO chemisorption were conducted. CO chemisorption gave slightly higher metal dispersion than H_2 chemisorption on Rh catalysts. The Ni metal dispersion value seems low by both CO and H_2 chemisorption analysis. Adding 2–10% Ni to 2% Rh by coimpregnation onto CeO_2–Al_2O_3 tended to affect the CO chemisorption slightly but had little impact on H_2 chemisorption of Rh. The pore volume values of the Rh and Rh–Ni were similar. The metal dispersion values allow the quantitative estimation of surface Rh among the total amount of Rh loaded. The Rh–Ni interactions were further examined by TPR and XPS results. We discuss these findings in detail later in the paper, but, briefly, TPR showed that the presence of Ni increased the temperature for Rh reduction, and XPS revealed that Rh helped maintain Ni in a reduced state in an oxidative atmosphere.

Table 1
Basic characterization of the catalysts prepared and examined

Catalyst	BET surface (m^2/g)	Pore volume (mL/g)	Metal dispersion (%)			
			Rh (CO)	Rh (H_2)	Ni (CO)	Ni (H_2)
2% Rh/CeAl	130.8	0.448	38.4	35.1	–	–
2% Rh–2% Ni/CeAl	118.9	0.428	41.6	34.0	6.0	4.3
2% Rh–5% Ni/CeAl	126.4	0.432	41.9	32.3	2.4	6.4
2% Rh–10% Ni/CeAl	115.8	0.365	34.9	36.7	2.1	7.9
10% Ni/CeAl	128.2	0.467	–	–	4.0	4.3
5% Ni/CeAl	124.5	0.692	–	–	4.5	1.9
2% Rh–5% Ni/Al_2O_3	148.0	0.728	52.1	46.2	1.9	8.2
5% Ni/Al_2O_3	157.5	0.918	–	–	3.5	1.8
2% Rh/Al_2O_3	156.6	0.953	–	–	–	–

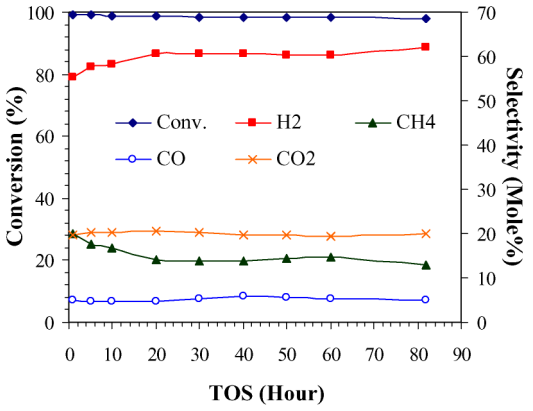

Fig. 1. Conversion and selectivity with 2 wt% Rh supported on 20% CeO_2–Al_2O_3 during reforming of MJF (model jet fuel) containing 20% aromatics.

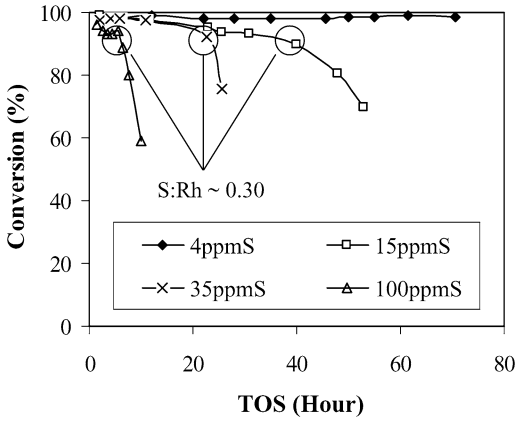

Fig. 2. Catalytic performance of 2% Rh supported on 20% CeO_2–Al_2O_3 for reforming of NORPAR-13 doped with 15, 35 and 100 ppm sulfur in the form of 3-methylbenzothiophene.

3.2. Reforming performance of Rh–CeAl

Fig. 1 shows the conversion and selectivity during reforming of the sulfur-free MJF over 2% Rh–CeAl for 83 h. From the first several hours to as long as 83 h of time on stream (TOS), MJF conversion was 98%, and product selectivity is near equilibrium with a dry gas composition of 61% H_2, 15% CH_4, 20% CO_2, and 4% CO with no traces of hydrocarbons other than those in the initial feedstock. TPO analysis of the spent catalyst found a total amount of carbon species of 3.06 wt%, mainly adsorbed hydrocarbons and highly amorphous carbon, as discussed elsewhere [38]. These initial studies of the Rh-based catalysts clearly show that Rh was highly active for the conversion of sulfur-free fuels, with little to no carbon formation during reforming at 512 °C, but that over alumina support, carbon formation increased slightly, to 3.98%. The main difference in the TPO profiles was an increase in more structured carbons that were not removed via TPD under nitrogen atmosphere for the alumina support. In previous studies, the decreased carbon with the addition of ceria on Ni catalysts was attributed to increased water adsorption on the support and improved oxygen storage leading to improved carbon gasification [12,39–41]. This implies that ceria helps decrease carbon formation on the Rh-based catalysts through the gasification of pyrolytic carbons and improved reforming of adsorbed carbon species, as seen with Ni-reforming catalysts. In addition, previous studies have indicated that ceria can aid in the stabilization of Rh dispersion and alumina support stability [42,43].

3.3. Effect of sulfur on Rh–CeAl

Evaluation of the sulfur tolerance of the supported Rh catalyst was conducted using NORPAR-13 with various concentrations of 3-methylbenzothiophene, as illustrated in Fig. 2. The original NORPAR-13 contained 4 ppm of sulfur. Reforming of the original NORPAR-13 over the Rh–CeAl catalyst showed high conversions and product stability for 72 h TOS, after which the Rh–CeAl showed no evident signs of deactivation, indicating that the Rh-based catalyst is sulfur-resistant to fuels containing <4 ppm of sulfur for at least 3 days. Increasing the sulfur content of the NORPAR-13 from 4 to 15 ppm led to a gradual deactivation at approximately 40 h TOS, after which deactivation becomes rapid. Similarly, with a further increase in the sulfur content of the NORPAR-13 to 35 ppm, gradual deactivation occurred until 21 h TOS, followed by rapid deactivation.

Table 2
Effect of sulfur on the final conversion, the fuel sulfur to surface rhodium ratios at deactivation of the reforming (S:Rh Refor.) and methanation (S:Rh CH_4) reaction, and the total amount of carbon species formed and/or adsorbed on the Rh-based catalysts during reforming of sulfur doped NORPAR-13 at 512 °C, 1 atm and S/C = 3

Catalyst	S conc. of NORPAR	Total TOS (h)	Final conversion	S:Rh[a] Refor.	S:Rh[a] CH_4	Carbon (wt%)
2% Rh/CeAl	4 ppm	72	96%	ND	ND	3.11
2% Rh/CeAl	15 ppm	57	70.2%	0.27	0.14	2.94
2% Rh/CeAl	35 ppm	25.5	75.5%	0.33	0.18	3.07
2% Rh/CeAl	100 ppm	10	58.8%	0.28	0.11	2.99
2% Rh/CeAl	33 ppm	44	3.8%	0.29	0.16	7.64[b]
2% Rh/Al	15 ppm	10	97.6%	NA	NA	3.89[b]

[a] Based on H_2 chemisorption.
[b] Higher temperature TPO peak associated with higher-order carbon.

As a quantitative estimate of sulfur tolerance of the catalyst to the amount of sulfur in fuel flow over the catalyst bed, Table 2 gives the sulfur in fuel-to-surface-Rh atomic ratio (S:Rh Refor. meaning S_{fuel}:Rh_{surf}) at the onset of the rapid deactivation of the reforming activity. The calculated S_{fuel}:Rh_{surf} ratio at the point of rapid loss in conversion was 0.30 ± 0.03 (the amount of surface Rh estimated based on H_2 chemisorption data) or 0.27 ± 0.03 (the amount of surface Rh estimated based on CO adsorption data). The rapid deactivation occurring at an approximate S_{fuel}:Rh_{surf} ratio of 0.30 held even when the sulfur content was increased to 100 ppm.

Evaluation of the onset of rapid deactivation clearly indicates that the amount of sulfur in the initial fuel had little impact on conversion before reaching a S_{fuel}:Rh_{surf} ratio of about 0.30. This implies that the activity is affected by the level of sulfur poisoning, rather than by the amount of sulfur initially in the fuel. Furthermore, the amount of carbon deposition is unaffected by the amount of sulfur originally present in the fuel or

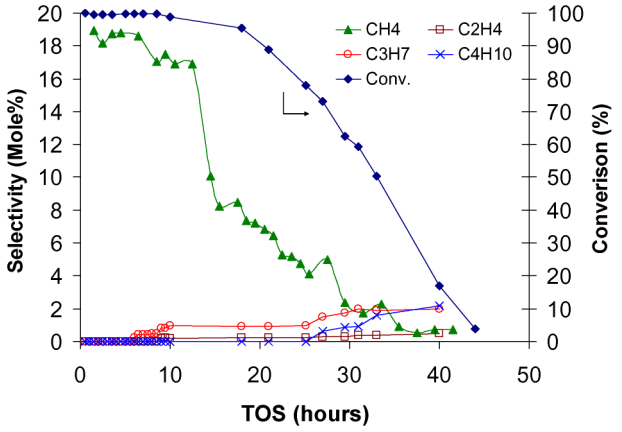

Fig. 3. Conversion of 33 ppmS NORPAR-13 over 2% Rh/CeO_2–Al_2O_3 catalyst and selectivity for the production of methane, ethylene, propane and butane during reforming at 512 °C, 1 atm and S/C = 3.

the TOS as long as the reaction is terminated prior to extensive deactivation, as given in Table 2.

Fig. 3 shows the conversion and methane selectivity during steam reforming of the sulfur-doped NORPAR-13 under the same conditions over the Rh–CeAl catalyst, but with the catalyst kept on stream till minimal activity was observed. In addition to conversion and methane selectivity, Fig. 3 also shows the formation of ethylene, propane, and butane. Similar to the results from testing with 35 ppm NORPAR-13, slow deactivation of the catalyst occurred after ∼10 h and rapid deactivation occurred after ∼20 h. Once a high level of sulfur poisoning of the catalyst occurred, the activity approached zero and pyrolysis of the fuel became the predominant pathway [2], resulting in the formation of C_2 and higher olefins and paraffins. Once the catalyst reached significant deactivation, significant carbon formation occurred on the catalyst (Table 2).

Delahay and Duprez [32] studied the effect of sulfur on coking during steam reforming of methylnaphthalene over Rh–Al_2O_3 catalysts and proposed two hypotheses: (i) Increased coking results from adsorption of sulfur species and subsequent decomposition of the sulfur species, and (ii) sulfur inhibits the carbon-to-steam reaction that prevents the Rh from reforming carbon species on the surface or coke precursors [32]. In that study the reaction time was constant, and thus the level of sulfur poisoning was not. Holding the reaction time constant (3 h), the authors found that higher sulfur content led to increased coke production and that sulfur species coexisted with the coke on the catalyst. But poisoning of the Rh active sites would lead to polymerization and the inability of Rh to gasify carbon deposited from pyrolytic carbon (and coke precursors) due to retardation of the carbon-to-steam reaction. If this were to occur, then increasing the surface coverage of sulfur would lead to higher carbon formation levels as with increasing sulfur coverage and would produce the same results observed by Delahay and Duprez.

Our investigation of the effects of sulfur and carbon on the deactivation of the Rh catalysts at similar levels of deactivation indicated that sulfur poisoning was the main route to the deactivation of the active sites, whereas carbon formation on the catalyst contributed to the catalyst deactivation only after significant sulfur poisoning. Our evidence supports the second hypothesis of Delahay and Duprez, that sulfur inhibits the steam-to-carbon reaction, with the modification that the impact of sulfur on coking is independent of the sulfur concentration of the fuel; rather, carbon formation is dependent on the degree of sulfur poisoning of the catalyst (i.e., surface coverage of the Rh metal).

The influence of sulfur poisoning on methanation reactions is more profound than that on the carbon-to-steam reactions over traditional Ni-based catalysts [29]. We observed the same trend over Rh-based catalysts, where the production of methane was affected before the loss of fuel conversion in the presence of sulfur. The methane formation (methanation) reactions include hydrogenation of CO and CH_x from CO, as well as CH_x from cleavage of CH_x–CH_y bonds in hydrocarbons in this study. At S_{fuel}:Rh_{surf} ratios of 0.13–0.15 (0.15 ± 0.04 based on H_2 pulse chemisorption data or 0.13 ± 0.03 based on CO chemisorption data), methane selectivity began to decline at a constant rate for reforming of 15, 35, and 100 ppm NORPAR-13 over the Rh–CeAl catalyst. (No deactivation of the methanation reaction was observed for reforming of 4 ppm NORPAR-13.)

Recent theoretical studies of S adsorption on Rh(111) surfaces found that S coverage of 1:9 can affect the ability to adsorb CO [44]. This finding is in good agreement with previous studies on sulfur poisoning of Ni-based catalysts for methanation of CO in H_2 [45]. Earley and Wagner reported that each sulfur atom blocks about nine CO adsorption sites on the Ni(111) surface, hindering the initial CO methanation step of CO on the Ni(111) surface. CH_4 formation in the present work may come from two different routes: direct formation of methane from C–C bond cleavage of higher hydrocarbons and methanation of CO product by the H_2 product. The present study with Rh–CeAl catalysts shows that methane formation started to be hindered at a S_{fuel}:Rh_{surf} ratio of approximately 0.15, in close agreement with the value found for Ni catalysts. Fig. 3 shows that the production of methane practically stopped at 34 h TOS and corresponded to a S_{fuel}:Rh_{surf} ratio of 0.45, indicating that the methanation reactions, particularly CO adsorption, also stopped. Erley and Wagner reported that at sulfur coverages of 0.33, CO adsorption on Ni(111) surfaces stopped completely for the conditions studied [45] and was about 3 times that of the initial retardation of CO adsorption. In the current study, the S_{fuel}:Rh_{surf} ratio of 0.45 corresponded to about 2.8 times the ratio of observed initial retardation in the methanation reaction, very similar to the findings of Erley and Wagner on Ni(111), thus implying that methanation on Rh-based catalysts requires an ensemble size similar to that of Ni.

3.4. Effect of Ni addition on sulfur resistance of Rh–CeAl

Protecting the Rh active sites from sulfur adsorption is critical to improving the sulfur resistance of Rh-based catalysts. Our preliminary work indicated that adding Ni to Rh is a promising approach to accomplish this goal. It is well known that sulfur will adsorb onto Ni; furthermore, Ni is active for the steam reforming of hydrocarbon fuels. The impact of Ni addition dur-

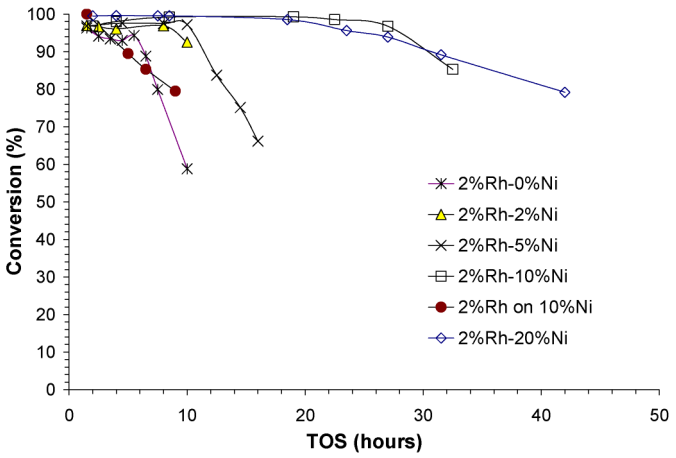

Fig. 4. Catalytic conversion profiles for steam reforming of 100 ppmS NORPAR-13 and the effect of Ni loading level on the sulfur tolerance of 2% Rh–X% Ni/CeO_2–Al_2O_3 catalyst. $X = 0$, 2, 5, 10 and 20 wt%. For additional comparison, a catalyst with 2% Rh loaded on calcined 10% Ni/CeO_2–Al_2O_3 is also presented (2% Rh on 10% Ni).

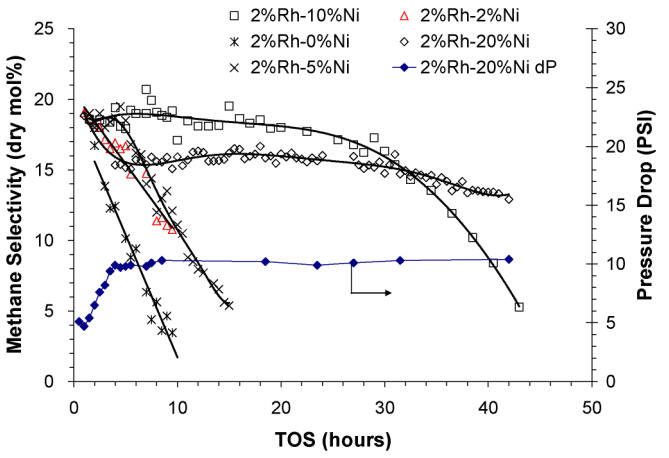

Fig. 5. Methane selectivity during steam reforming of 100 ppmS NORPAR-13 over 2% Rh–X% Ni/CeO_2–Al_2O_3 with $X = 0$, 2, 5, 10 and 20 wt%; including the pressure drop for 2% Rh–20% Ni.

ing reforming of 100 ppmS NORPAR-13 is shown in Fig. 4. Combining 2 wt% Ni with the Rh during loading led to improved sulfur resistance via an increase in the TOS from 5 to 8 h before rapid deactivation of the reforming reactions. For a Ni content of 5 wt%, further improvement in sulfur tolerance of the catalyst during reforming of 126 ppmS NORPAR-13 resulted from increasing the time of stability to 10 h. Adding 10 wt% Ni to the Rh-based catalyst led to a dramatic improvement in the sulfur resistance of the catalyst; >95% conversion was maintained for up to 28 h during reforming of 100 ppmS NORPAR-13.

Further increases in Ni content beyond 10% did not further improve catalytic performance, as shown in Fig. 4, where steady deactivation began after 19 h and steadily dropped to 78% conversion after 42 h when 20% Ni was incorporated with 2% Rh. The earlier onset of deactivation and the steady trend in deactivation for the 2Rh20Ni–CeAl catalyst were due largely to significant carbon formation, as implied by the high level of carbon deposits and increased pressure drop across the catalyst bed.

Examining the methanation reaction can provide insight into the level of deactivation by sulfur poisoning. The methanation reaction is generally more sensitive to sulfur poisoning than reforming reactions, as has been reported previously [29].

Fig. 5 shows the selectivity of methane for reforming of 100 ppmS NORPAR-13 with various Ni loadings. When no Ni was loaded onto the catalyst, a rapid loss in methane selectivity occurred, with a methane/TOS slope of approximately −1.7. Adding 2% Ni again caused a rapid drop in methane selectivity during reforming of 100 ppmS NORPAR-13. For 2% Ni loadings, the calculated slope of the loss in methane selectivity improved slightly to −1, and at around 3–5 h TOS a slight leveling of the slope occurred before continued deactivation. The loss of methane selectivity implied that adding 2% Ni slowed the poisoning effect of sulfur by nearly a factor of two.

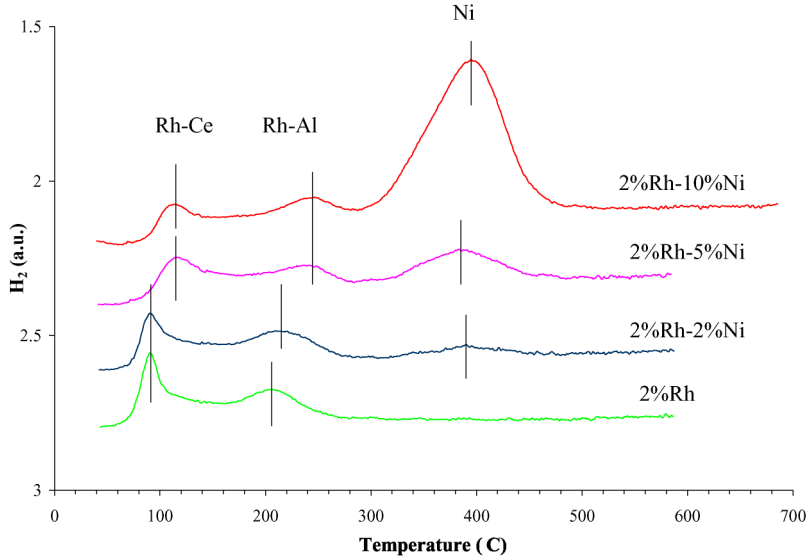

Fig. 6. TPR profiles of 2% Rh co-loaded with 2, 5 and 10% Ni supported on 20% CeO_2–γ-Al_2O_3.

The TPR profiles in Fig. 6 indicate that at 2% Ni loading there was very limited interaction of Rh–Ce with Ni and implies that protection of Rh–Ce would not be achieved by adding Ni, as discussed below. TPR did reveal a slight interaction with Rh–Al and Ni, which may the reason for the slight leveling of methane deactivation at 3–5 h. The decreased slope of methane production implies that both the Rh and Ni will deactivate in the presence of sulfur, with the only benefit of Ni addition being to serve as a sacrificial site to adsorb some sulfur. Support for the improved performance as a result of adding Ni sacrificial sites is provided by the fact that reforming was significantly hindered once a S_{fuel}:Rh_{surf} ratio of 0.35 was reached for the 2Rh2Ni–CeAl catalyst. This is only slightly higher than the ratio of 0.30 observed for Rh–CeAl catalyst and can be attributed to some sulfur adsorption on the Ni metal. Furthermore, the S_{fuel}:Rh_{surf} ratio for the decrease in methanation was approximately 0.13, in good agreement with the calculated ratio for methanation hindrance over Rh–CeAl.

Adding 5 and 10% Ni stabilized methane production for 6 and 28 h, respectively, after which rapid deactivation of the methanation reaction occurs. For the 2Rh20Ni–CeAl catalyst, methane production initially began to fall and then stabilized at 17 mol%, and no rapid deactivation of the methanation reaction was observed. The initial drop in methane selectivity to the same selectivity level of the catalysts containing only Rh implies that Ni did not significantly contribute to methanation reactions. The increased pressure drop with reduced methane selectivity implies that for 20% Ni loading, the decreased methane selectivity can be attributed to carbon formation. Because methane production did not decrease rapidly for the 20% Ni catalyst and fuel conversion dropped, deactivation of the reforming reactions most likely occurred due to carbon formation, rather than sulfur poisoning. Although deactivation occurred in the reforming reactions, methane selectivity remained nearly constant for 20% Ni loading, at the same level as seen for reforming of the sulfur-free MJF, implying that the Rh was still being protected by the addition of Ni. With Ni loadings of 0, 2, and 5 wt%, deactivation was due mainly to sulfur poisoning, not carbon formation. Deactivation due to sulfur poisoning for low Ni loadings can be confirmed by the minimal carbon deposition on the catalyst and the rapid decrease in the sulfur-sensitive methanation reaction. In the case of 10% Ni loadings, the methanation reaction was deactivated at around the same time that the loss in conversion occurred. Considering the high amount of carbon formed on the 2Rh20Ni–CeAl catalyst, the loss in conversion is due to carbon formation, not to sulfur poisoning.

3.5. Influence of the method of Ni addition to Rh–CeAl on the sulfur resistance

To verify the importance of close interaction in the Rh–Ni prepared by coimpregnation in this work, we also prepared and tested an additional catalyst of 2% Rh and 10% Ni supported on CeAl. The preparation of this catalyst differed in that the Rh was loaded onto calcined Ni–CeAl (after the Ni was loaded on the CeAl and calcined at 500 °C). Fig. 4 presents the results of this test and compares them to results of testing the 2Rh10Ni–CeAl prepared by coimpregnating the Rh and Ni onto the CeAl. As seen in Fig. 4, there was a steady drop in the conversion of 126 ppmS NORPAR-13 with no measurable period of stability. The slope of deactivation was −2.75, considerably slower than that of deactivation of 2Rh–CeAl. Without the close contact between Ni and Rh afforded by the coimpregnation preparation method, there is no prolonged period of stability, implying that the Ni is not protecting the Rh from sulfur poisoning. The lack of steady conversion and the significant rate of deactivation from almost the beginning of TOS imply that in this catalyst Rh was not functioning as an effective catalytic component and Ni may have been acting only as a sulfur sacrificial site (for Rh) in a similar way as the Ni in the 2Rh2Ni–CeAl catalyst. Thus in this case the Rh–Ni interaction was different (if existing at all) and did not provide any significant Rh protection.

3.6. Rh–Ni interaction by TPR analysis and comparative reforming tests

Fig. 6 shows the TPR profiles of Rh supported on ceria–alumina with 0, 2, 5, and 10% Ni loadings. For the monometallic Rh catalyst, two peaks at 89 and 203 °C can be attributed to Rh associated with ceria (Rh–Ce) and alumina (Rh–Al), respectively. This is similar to the findings reported by Hou and Yahima [46]. For the 2Rh2Ni–CeAl catalyst, a broad third peak appeared at 387 °C attributed to the reduction of NiO. In addition to a peak for Ni, 2% Ni loading produced a slight shift in the Rh–Al peak to a higher temperature of 213 °C. Increasing the Ni loading to 5 and 10% caused further shifts in the Rh–Ce and Rh–Al peaks to 109 °C and 242 °C, respectively. This implies a more intimate contact between the Ni and Rh at the higher Ni loadings. The TPR data indicate that most of the Rh metal was associated with Ni for Ni loadings of 5 and 10%.

At rapid deactivation of the methanation reaction, the calculated S_{fuel}:Ni_{surf} ratio, as given in Table 3, was nearly constant at 0.58 and 0.60 for 5% and 10% Ni loadings, respectively. The corresponding S_{fuel}:Rh_{surf} ratios for both catalysts are higher than that for the supported catalyst containing only Rh; this further implies that the Ni addition is the reason for improved sulfur tolerance. Rostrup-Nielsen found that for various Ni-reforming catalysts, Ni saturation occurred at a S_{fuel}:Ni_{surf} ratio of approximately 0.54 [47]. The observed S_{fuel}:Ni_{surf} values at the retardation of the methanation reactions observed in this study are close to those reported by Rostrup-Nielsen for Ni. Because on Rh–CeAl catalyst methanation reactions rapidly decrease during reforming of 100 ppmS NORPAR-13, we can postulate that the Ni protects the Rh metal from poisoning until Ni saturation occurs.

We performed a third test to gain insight into the role of Ni addition, involving reforming of 100 ppmS NORPAR-13 over 2% Rh–5% Ni supported on alumina (2Rh5Ni–Al). We found that the activity of the 2Rh5Ni–Al catalyst was similar to that of 2Rh5Ni–CeAl, and methanation reactions underwent rapid deactivation at a S_{fuel}:Ni_{surf} ratio of 0.54. This implies that the ceria may make a slight contribution to improved sulfur uptake by the Ni metal or improved sulfur resistance of the Rh. Al-

Table 3
Results of reforming of model fuels doped with sulfur over various catalysts

Catalyst	S conc. of NORPAR	TOS	Initial/final conversion	S:Ni/S:Rh Refor.	S:Ni/S:Rh CH_4	Carbon (wt%)
2% Rh/CeAl	100 ppm	10	100/59	–/0.28	–/0.11	2.99
2% Rh–2% Ni/CeAl	100 ppm	10	98/92	1.6/0.35	0.40/0.13	3.06
2% Rh–5% Ni/CeAl	126 ppm	16	99/66	0.77/0.67	0.58/0.52	2.96
2% Rh–10% Ni/CeAl	100 ppm	32	100/65	0.60/1.1[a]	0.60/1.1	24.7[b]
2% Rh + 10% Ni/CeAl	126 ppm	9	100/75	0.46/0.22[c]	0.22/0.11[c]	8.21[c]
2% Rh–20% Ni/CeAl	126 ppm	42	98/78	0.29 (0.62)/1.2 (2.3)[d]	0.50 (0.62)/1.9 (2.3)[d]	34.4[b]
2% Rh–5% Ni/Al	104 ppm	19	100/71	0.68/0.54	0.54/0.42	4.89[e]
5% Ni/Al	33 ppm	4.5	80/5	NA[f]	NA[f]	13.7[b,e]
5% Ni/CeAl	104 ppm	3.5	98/35	NA[f]	NA[f]	14.9[b]
10% Ni/CeAl	104 ppm	5	95/98	NA[f,g]	NA[f,g]	59.9[g]

[a] Carbon deposition also contributed to deactivation, in addition to sulfur poisoning.
[b] Mainly filamental carbon, with some amorphous carbon.
[c] For 2% Rh loaded on precalcined 10% Ni/CeAl and tested for 9 h TOS.
[d] For S:metal ratios at the first inflection point for deactivation (and those at the end of test TOS).
[e] Significant amorphous carbon deposited on catalyst.
[f] No stable reforming period.
[g] Major carbon deposition caused reactor plugging; pressure drop exceeded 60 psi and catalyst/carbon agglomerates and catalyst particle disintegration observed.

though a minor improvement in sulfur tolerance occurred in the presence of ceria, the main benefit of ceria addition was reduced carbon formation for Rh, Ni, and Rh–Ni catalyst, as shown in Table 3.

Efforts were made to calculate the S_{fuel}:Ni_{surf} ratios at rapid deactivation of the methanation and reforming reactions over Ni–CeAl and Ni–Al catalysts, as shown in Table 3. For the 5Ni–Al catalyst, rapid deactivation occurred for both the methanation and reforming reactions. Although adding ceria to the support improved the conversion and stability of the reforming reactions, no period of stability was observed. The effect of ceria on carbon formation is a reduction in amorphous pyrolytic carbons. For the 5Ni–CeAl catalyst the main carbon species can be attributed to ordered/filamentous carbons; while for the 5Ni–Al catalyst both amorphous and ordered/filamentous carbons were detected. This suggests that ceria improved the gasification of pyrolytic carbons deposited on the catalyst. The slightly improved stability of the 5Ni–CeAl catalyst was due to less pyrolytic carbon, which can encapsulate the active Ni. For the 10Ni–CeAl catalyst, high activity was noted, but extensive carbon formation led to the formation of a carbon/catalyst plug in the reactor. The pressure in the reactor increased to 60 psi, and the reaction had to be terminated. Thus, under the conditions used in the present study, the use of Ni alone as a reforming catalyst is not practical, due to extensive carbon formation, and comparing our findings with those of other studies is difficult due to the drastic increase in pressure in the system. The use of a bimetallic Rh–Ni catalyst is superior in terms of lower carbon formation, better activity and stability over monometallic Ni catalysts, and higher sulfur resistance over monometallic Rh catalysts.

3.7. XPS of Rh–Ni on CeAl

We further examined the Rh–Ni interaction observed on TPR by conducting XPS analyses. Fig. 7 presents the Rh 3d XP spectra for 2Rh–CeAl, 2Rh2Ni–CeAl, and 2Rh5Ni–CeAl

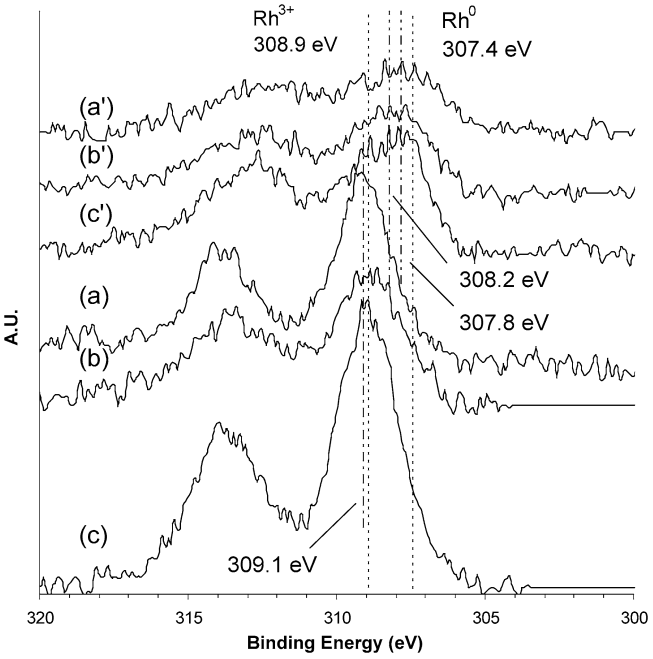

Fig. 7. Normalized Rh 3d XP spectra for (a) 2% Rh–5% Ni–CeAl, (b) 2% Rh–2% Ni–CeAl, (c) 2% Rh–CeAl after calcination and (a′) 2% Rh–5% Ni–CeAl, (b′) 2% Rh–2% Ni–CeAl, (c′) 2% Rh–CeAl after reduction and air exposure for 24 h.

after calcinations and after reduction followed by air exposure for 24 h. The calcined 2Rh–CeAl and 2Rh2Ni–CeAl catalysts exhibited similar Rh 3d peak shapes and an FWHM position of 308.9 eV, corresponding to the presence of Rh^{3+} [48] and FWHMs of 2.6 and 2.2, respectively. For the 2Rh5Ni–CeAl, there was a minor shift of about 0.2 eV, corresponding to an FWHM position of 309.1 eV and an FWHM of 2.19 eV. Such a slight shift was also reported by Nefedov et al. for $NiRh_2O_4$; these authors found FWHM positions of 308.9 for Rh_2O_3 and 309.0 for $NiRh_2O_4$. We observed this same shift trend in the present study, which may imply the

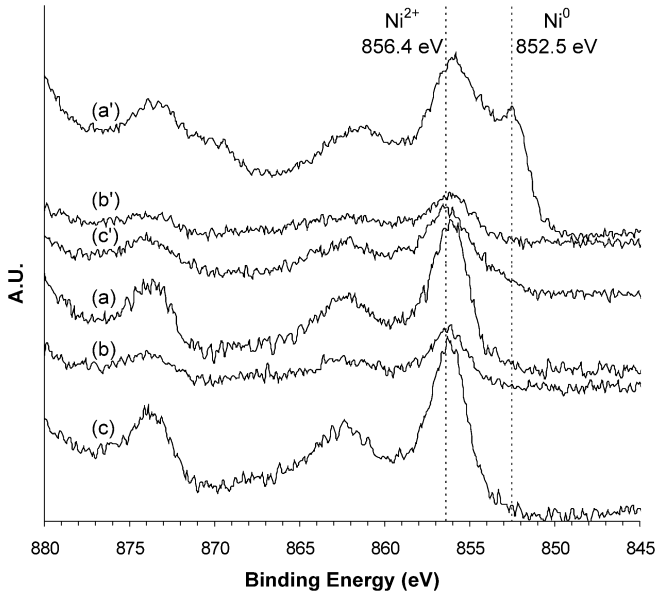

Fig. 8. Normalized (based on max intensity) Ni 2p XP spectra for (a) 2% Rh–5% Ni–CeAl, (b) 2% Rh–2% Ni–CeAl, (c) 5% Ni–CeAl after calcination and (a′) 2% Rh–5% Ni/CeAl, (b′) 2% Rh–2% Ni/CeAl, (c′) 5% Ni/CeAl after reduction and air exposure for 24 h.

presence of a Ni–Rh oxide species in the 2Rh5Ni–CeAl catalyst.

After reduction and exposure to air, a clear shift and a broadening of the Rh 3d peak shapes occurred. Kugai and co-workers found that Rh^{3+} was completely reduced to Rh^0 after reduction, but after exposure to air for only 3 min, a mix of Rh^{3+} and Rh^0 was present in Rh–Ni supported on CeO_2 [49,50]. In the present study we have observed a similar phenomena, in that after reduction, most of the Rh was in a metallic phase, and after air exposure for 24 h, partial oxidation of the Rh metal back to Rh^{3+} occurred. Support for this assumption is given in Fig. 9, where after calcination, the binding energy is 308.9 eV, and after reduction and air exposure, the binding energy is approximately 308.2 eV (for 2Rh–CeAl and 2Rh2Ni–CeAl). These findings are consistent with those of Kugai and co-workers, who found a binding energy of air-exposed reduced Rh on CeO_2 of 308.1 eV and reported that any Rh remaining in the metallic phase would be expected to have a binding energy at a FWHM position of approximately 307.4 eV [49–51]. The position of the FWHM of the 2Rh5Ni–CeAl sample after reduction and air exposure is 307.8 eV. The lower binding energy signifies that more of the Rh is remaining in the metallic phase after air exposure and implies that there could exist a possible interaction with Ni. The present results indicate that there exists a close interaction between the Rh and Ni, although we do not have the conclusive evidence for Rh–Ni alloy formation in the catalyst.

Fig. 8 presents the Ni 2p XP spectra for 5Ni–CeAl, 2Rh2Ni–CeAl, and 2Rh5Ni–CeAl after calcinations and after reduction followed by air exposure. After calcination, the Ni 2p spectra for all samples have a binding energy of 856.2 eV, consistent with the Ni^{2+} oxidation state [48]. Only after reduction and air exposure was there an observable difference in the Ni 2p region. For both the 5Ni–CeAl and 2Rh2Ni–CeAl, there was little change to the Ni 2p region after reduction and air exposure. Kugai and co-workers observed nearly complete oxidation of surface Ni^0 back to Ni^{2+} after reduction and air exposure for 3 min [49,50], and our findings clearly show that any surface metallic Ni that may have formed during reduction was converted back to Ni^{2+} after 24 h of exposure to air at room temperature. However, for the 2Rh5Ni–CeAl sample, there was significant retention of surface metallic Ni after air exposure. This implies the presence of a strong interaction in surface Rh–Ni species that is keeping the Ni in the metallic state instead of oxidizing back to Ni^{2+}. In a previous study of Rh–Ni supported on γ-alumina, Leclercq and co-workers found that after reduction at 900 °C, "surface enrichment" of Ni occurred corresponding to a binding energy of 852.5 eV [52]. In the current study, the FWHM position of the second peak found in the Ni 2p spectra was 852.6 eV, consistent with the study by Leclercq et al. and the value for Ni^0 reported by Kugai et al.

Considering the Ni 2p and Rh 3d XP spectra for 2Rh5Ni–CeAl, a close interaction between the Rh and Ni phases clearly exists that is consistent with the above-mentioned TPR data. In addition to XPS and TPR evidence for a Rh–Ni interaction, the chemisorption data for the 2Rh5Ni–CeAl (and 2Rh10Ni–CeAl) also indicate a Rh–Ni interaction. As shown in Table 1, adding Ni with Rh to CeAl caused a steady increase in hydrogen dispersion from 4.3 to 7.9 for 2Rh2Ni–CeAl and 2Rh10Ni–CeAl, respectively. However, the calculated CO dispersion for Ni dropped significantly with the addition of 5 and 10% Ni with Rh to CeAl. The Ni dispersion based on CO adsorption was 6.0% for the 2Rh2Ni–CeAl sample and 2.4% for the 2Rh5Ni–CeAl sample. CO will typically adsorb linearly on Ni surfaces at low surface coverage, and multiple CO bonding to single Ni atoms may also occur [53]. FTIR studies of Rh–Ni supported on SiO_2 showed that Ni addition caused the Rh to lose bridge-formed CO adsorption sites [54]. If this were indeed the case in the current study, then we would expect the CO calculated dispersion to increase rather than decrease with Ni loadings of 5 and 10%. Jozwiak et al. used significantly different ratios of Rh and Ni than we used in the current study and reported different phases of Rh–Ni based on the preparation and support differences. In the current study, the reduced CO adsorption may imply a decrease in subcarbonyl species (two to three linearly bonded CO molecules) on Ni sites or a possible interaction with Rh that could result in the possibility of CO being able to bond on bridge sites of a Rh–Ni bimetallic species. Further analysis by FTIR is needed to identify the cause of the inverse relationship to the dispersion calculation for CO and the dispersion calculation for H_2. At this time, we can only hypothesize that a Rh–Ni interaction is the cause of decreased CO adsorption for Rh–Ni catalysts with Ni loadings of 5% or more, while H_2 adsorption increases. However, considering the XPS and TPR results, this is not an unreasonable speculation.

3.8. Role of Ni for protecting Rh in Rh–Ni–CeAl

The present experimental and analytical results suggest that there exist strong Rh–Ni interactions on adding nickel to the rhodium by the coimpregnation preparation method used in

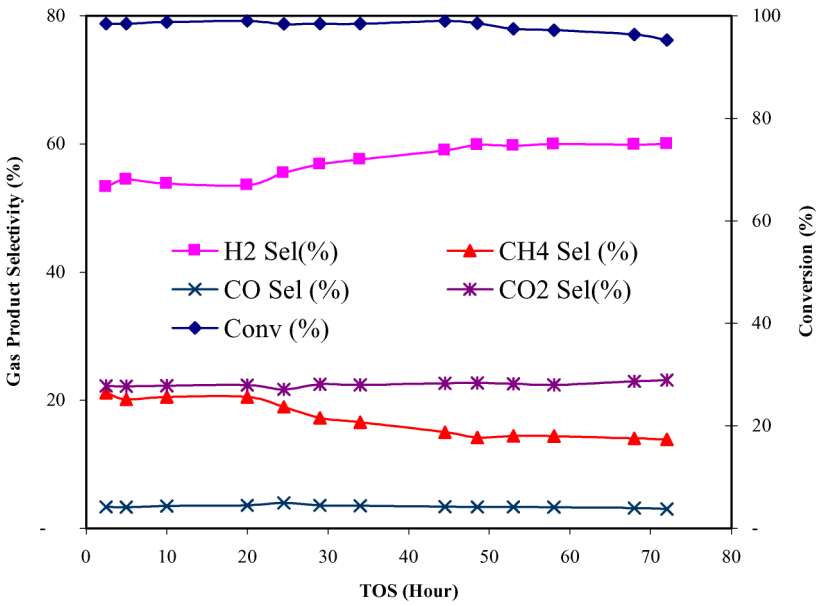

Fig. 9. Selectivity and conversion during reforming of a desulfurized JP-8 over 2% Rh–10% Ni–CeAl (2% Rh–10% Ni/CeO_2–Al_2O_3) for 72 h.

this work. This finding is consistent with the low-temperature reforming results that the Ni is protecting the Rh rather than merely acting as a sacrificial site, when using the coimpregnation of Rh and Ni salts onto CeO_2–Al_2O_3 support. The additional results with a two-step preparation in which 2% Rh is added onto precalcined 10% Ni/CeO_2–Al_2O_3 clearly (see Fig. 4 for 2% Rh on 10% Ni) showed that the above-mentioned desirable effect of Ni protecting Rh is not observed when Ni and Rh are not in close vicinity.

It is proposed that the Ni closely interacts with Rh metal and protects Rh from sulfur poisoning through two possible mechanisms. First, Rh species are surrounded by Ni species in close vicinity (when prepared by coimpregnation onto CeO_2–Al_2O_3), and Ni reacts preferentially with sulfur. Thus Rh can largely remain active for steam reforming in the presence of sulfur. Second, when some Rh atoms do react with sulfur, such sulfur in RhS_x can transfer to Ni present in the close vicinity of Rh. S in RhS_x may be transferred to the Ni metal through sulfur spillover with or without the aid of gas-phase hydrogen. The presence of reducing gas such as H_2 in the gas phase may aid the sulfur spillover via H_2S; that is, H_2S formed from reaction of RhS_x with H_2 can react with Ni to form NiS_x, thus shifting the equilibrium toward NiSx, because a larger number of Ni atoms are present in the vicinity of Rh. In other words, a possible sequence of reaction that can lead to sulfur spillover from Rh–S to Ni–S under H_2 is $Rh–S + H_2 = Rh + H_2S$; $Ni + H_2S = NiS + H_2$, with the net reaction appearing as $Rh–S + Ni = Rh + Ni–S$. Confirmation of this sequence requires further study, however. In either case, a close interaction between the added Ni and Rh is necessary for protection of the Rh. Supporting evidence for Rh and Ni interactions have been obtained by TPR and XPS analysis, which supports the hypothesis that Ni protects Rh through a close Rh–Ni interaction. We do not have clear evidence whether or not Ni and Rh form an alloy in the present catalyst system, but clearly a very close interaction does exist.

3.9. *Reforming of JP-8 jet fuel over Rh–Ni–CeAl*

Fig. 9 shows the reforming of a JP-8 jet fuel that has been desulfurized from nearly 400 ppm to 22 ppm using selective sulfur adsorption [17,18,21,23,24]. The liquid fuel conversion is nearly 100% for the initial 45 h, after which it decreases slightly to around 95% after 72 h TOS. The methane production drops slightly at approximately 20 h TOS before leveling off. A slight decrease in methane selectivity before leveling off was also observed during reforming of 100 ppmS NORPAR-13 over 2Rh20Ni–CeAl, which can be attributed to carbon formation hindering the improved methanation reactions over Ni metal. After the initial drop in methane production, the selectivities of methane and other product gases remain stable, implying that sulfur poisoning has not yet occurred on the Rh metal. At 72 h TOS, the S_{fuel}:Ni_{surf} is 0.36. If the proposed model is accurate and carbon formation is controlled, then rapid deactivation of the methanation reaction after approximately 110–120 h TOS would be expected as a result of Ni saturation by sulfur.

Although the catalyst did not show signs of Rh poisoning by sulfur, the conversion began to decrease after 45 h TOS, indicating another deactivation mechanism. TPO analysis showed that 15.8 wt% carbon was formed on the catalyst. The TPO profile of the CO_2 production from the carbon indicates significant amorphous pyrolytic carbon formation and deposition on the surface, which can lead to catalyst deactivations. During reforming of JP-8, there was less carbon deposition on the catalyst during reforming when compared to the reforming of NORPAR-13. Furthermore, the carbon formed from reforming of NORPAR-13 contained more filamentous carbon and less pyrolytic carbon. The difference in the carbon structure and the amount of carbon can be attributed to an increase in gas-phase carbon due to the presence of aromatics and alkyl-benzenes in the JP-8 [55–57]. Increased gas-phase carbon formation will increase the lay-down of carbon on the surface and can lead to the

formation of encapsulating carbon, which will prevent further formation and growth of filaments [58].

4. Conclusion

Rh on CeO_2-modified Al_2O_3 support can be used for low-temperature steam reforming of liquid fuels at $<520\,^{\circ}C$. With properly prepared Rh catalysts such as $Rh/CeO_2–Al_2O_3$, effective steam reforming of desulfurized jet fuels (<5 ppmw S) can be achieved at $<520\,^{\circ}C$ with >97% conversion to syngas and CH_4 for solid oxide fuel cell applications. Evaluation of the sulfur tolerance of the 2% Rh–CeAl catalyst showed a rapid decrease in conversion at a S_{fuel}:Rh_{surf} ratio of 0.30 and a decline in methane production over the catalyst starting at a S_{fuel}:Rh_{surf} ratio of 0.15, implying that methanation is about twice as sensitive to sulfur poisoning on Rh-based catalysts.

Although the concentration of sulfur in the fuel has a significant impact on the longevity of the Rh-based catalyst, it has no impact on the amount of carbon formed on the catalyst when the reaction is terminated before extensive poisoning. Carbon formation on the catalyst is a function of the degree of poisoning, rather than of the amount of sulfur in the fuel.

The addition of Ni to the Rh-based catalyst can greatly enhance the performance of the catalyst in the presence of sulfur. With only 2% Ni loadings, minimal Rh–Ni interactions lead to Ni serving only as a sacrificial sulfur adsorption site, resulting in minimal improvement in the deactivation of methanation reactions. The addition of 5 and 10% Ni to the Rh–CeAl exhibited strong Rh–Ni interactions that allowed the Ni to protect the Rh metal until Ni surface saturation was reached.

Once a S_{fuel}:Ni_{surf} of approximately 0.59 (for CeAl supported catalysts) was reached, rapid deactivation of the methanation reaction was observed. This implies that the methanation (and reforming) over Rh remains unaffected by sulfur until Ni saturation is reached.

Clearly, the addition of Ni can successfully protect the Rh metal when using the support and preparation method specified in this work. We propose that the Ni closely interacts with Rh metal and protects Rh from sulfur poisoning through two possible mechanisms. First, when Ni reacts preferentially with sulfur, the Rh can remain active for steam reforming. Second, when some Rh atoms do react with sulfur, such sulfur can transfer from Rh to Ni present in the close vicinity of Rh. In other words, S in RhS_x may be transferred to the Ni metal through sulfur spillover with or without the aid of gas-phase hydrogen. In either case, a close interaction between the added Ni and Rh is necessary. Evidence of Rh and Ni interactions obtained by TPR and XPS analysis supports the hypothesis that Ni protects Rh through a close Rh–Ni interaction.

The catalyst developed in this work, 2% Rh–10% Ni supported on CeO_2-modified Al_2O_3, shows excellent promise as a catalyst that can successfully reform sulfur-containing liquid hydrocarbons, such as jet fuel, as demonstrated by the reforming of JP-8 containing 22 ppm sulfur for 3 days TOS with >95% conversion.

Acknowledgments

The authors thank the Palm Power Program of US DoD/DARPA for sponsoring this study through a subcontract from Altex Technologies Corp, Mathew Hoehn and Todd Brieck for assistance in the reforming experiments, and Bob Hengstebeck of PSU Materials Characterization Laboratory for assistance in XPS analysis. They also thank Dr. Harold H. Schobert of PSU for helpful discussions and manuscript editing, Shingo Watanabe for assistance with BET measurements, and Dr. Mehdi Namazian and Siva Sethuraman of Altex Technologies for providing a fractionated jet fuel sample and for helpful discussions. Chunshan Song thanks the U.S. State Department and the U.S.–U.K. Fulbright Commission for the Fulbright Distinguished Scholar Award in conjunction with his sabbatical stay at Imperial College London, University of London.

References

[1] D.L. Trimm, Z.I. Onsan, Catal. Rev. - Sci. Eng. 43 (2001) 31.
[2] J.R. Rostrup-Nielsen, Phys. Chem. Chem. Phys. 3 (2001) 283.
[3] C.S. Song, Catal. Today 77 (2002) 17.
[4] R. Farrauto, S. Hwang, L. Shore, W. Ruettinger, J. Lampert, T. Giroux, Y. Liu, O. Ilinich, Ann. Rev. Mater. Res. 33 (2003) 1.
[5] J.R. Rostrup-Nielsen, Catal. Today 18 (1994) 305.
[6] J.R. Rostrup-Nielsen, Catal. Today 37 (1997) 225.
[7] J.N. Armor, Appl. Catal. A: Gen. 176 (1999) 159.
[8] J. Rostrup-Nielsen, D.L. Trimm, J. Catal. 48 (1977) 155.
[9] D.L. Trimm, Catal. Rev.-Sci. Eng. 16 (1977) 155.
[10] J.R. Rostrup-Nielsen, NATO ASI Ser., Ser. E: Appl. Sci. 54 (1982) 127.
[11] T. Borowiecki, A. Machocki, J. Ryczkowski, Stud. Surf. Sci. Catal. 88 (1994) 537.
[12] D.L. Trimm, Catal. Today 49 (1999) 3.
[13] J.R. Rostrup-Nielsen, T.S. Christensen, I. Dybkjaer, Stud. Surf. Sci. Catal. 113 (1998) 81.
[14] T.S. Christensen, Appl. Catal. A: Gen. 138 (1996) 285.
[15] J.H. Kim, X. Ma, C. Song, Y.K. Lee, S.T. Oyama, Energy Fuels 19 (2005) 353.
[16] S.T. Oyama, J. Catal. 216 (2003) 343.
[17] X. Ma, M. Sprague, C. Song, Ind. Eng. Chem. Res. 44 (2005) 5768.
[18] X. Ma, S. Velu, J.H. Kim, C. Song, Appl. Catal. B: Environ. 56 (2005) 137.
[19] X.L. Ma, L. Sun, C.S. Song, Catal. Today 77 (2002) 107.
[20] C.S. Song, Catal. Today 86 (2003) 211.
[21] C.S. Song, X. Ma, Appl. Catal. B: Environ. 41 (2003) 207.
[22] S. Velu, X. Ma, C.S. Song, Ind. Eng. Chem. Res. 42 (2003) 5293.
[23] S. Velu, X. Ma, C.S. Song, M. Namazian, S. Sethuraman, G. Venkataraman, Energy Fuels 19 (2005) 1116.
[24] S. Velu, C.S. Song, M.H. Engelhard, Y.-H. Chin, Ind. Eng. Chem. Res. 44 (2005) 5740.
[25] H. Topsoe, B.S. Clausen, F.E. Massoth, Hydrotreating Catalysis, Science and Technology, Springer, Berlin, 1996.
[26] D.D. Whitehurst, T. Isoda, I. Mochida, Adv. Catal. 42 (1998) 345.
[27] J.A. Babich, J.A. Moulijn, Fuel 82 (2003) 607.
[28] J.R. Rostrup-Nielsen, J. Catal. 21 (1971) 171.
[29] J.R. Rostrup-Nielsen, K. Pedersen, J. Catal. 59 (1979) 395.
[30] I. Alstrup, J.R. Rostrup-Nielsen, S. Roeen, Appl. Catal. 1 (1981) 303.
[31] J.R. Rostrup-Nielsen, NATO ASI Ser., Ser. E: Appl. Sci. 54 (1982) 209.
[32] G. Delahay, D. Duprez, Appl. Catal. 53 (1989) 95.
[33] D. Duprez, M. Mendez, J. Little, Appl. Catal. 27 (1986) 145.
[34] H.A. Yoon, M. Salmeron, G.A. Gomorjai, Surf. Sci. 395 (1998) 268.
[35] E.M. Yoon, L. Selvaraj, C.S. Song, J.B. Stallman, M.M. Coleman, Energy Fuels 10 (1996) 806.
[36] C.S. Song, W.-C. Lai, H.H. Schobert, Ind. Eng. Chem. Res. 33 (1994) 534.
[37] C.S. Song, X.L. Ma, Appl. Catal. B: Environ. 41 (2003) 207.

[38] J.J. Strohm, J. Zheng, C. Song, Prepr. Symp. - Am. Chem. Soc., Div. Fuel Chem. 48 (2003) 931.
[39] A. Trovarelli, C. de Leitenburg, G. Dolcetti, J.L. Lorca, J. Catal. 151 (1995) 111.
[40] A. Trovarelli, M. Boaro, E. Rocchini, C. de Leitenburg, G. Dolcetti, J. Alloys Comp. 323–324 (2001) 584.
[41] D.L. Trimm, Catal. Today 37 (1997) 233.
[42] R. Dictor, S. Roberts, J. Phys. Chem. 93 (1989) 5846.
[43] S. Kurungot, T. Yamaguchi, Catal. Lett. 92 (2004) 181.
[44] C.J. Zhang, P. Hu, M.H. Lee, Surf. Sci. 432 (1999) 305.
[45] W. Erley, H. Wagner, J. Catal. 53 (1978) 287.
[46] Z. Hou, T. Yashima, Catal. Lett. 89 (2003) 193.
[47] J.R. Rostrup-Nielsen, J. Catal. 11 (1968) 220.
[48] V.I. Nefedov, M.N. Firsov, I.S. Shaplygin, J. Electron Spectrosc. Relat. Phenom. 26 (1982) 65.
[49] J. Kugai, S. Velu, C.S. Song, J. Catal. Lett. 101 (2005) 255.
[50] J. Kugai, S. Velu, C. Song, M.H. Engelhard, Y.-H. Chin, Prepr. Pap. - Am. Chem. Soc., Div. Pet. Chem. 49 (2004) 346.
[51] Y. Abe, K. Kato, M. Kawamura, K. Sasaki, Surf. Sci. Spectra 8 (2001) 117.
[52] G. Leclercq, S. Pietrzyk, L. Gengembre, L. Leclercq, Appl. Catal. 27 (1986) 299.
[53] C.H. Rochester, R.J. Terrell, J. Chem. Soc., Faraday Trans. 73 (1977) 609.
[54] W.K. Jozwiak, M. Nowosielska, J. Rynkowski, Appl. Catal. A: Gen. 280 (2005) 233.
[55] C.S. Song, Y. Peng, H. Jiang, H.H. Schobert, Am. Chem. Soc., Div. Pet. Chem. Prepr. 37 (1992) 484.
[56] C.S. Song, W.-C. Lai, H.H. Schobert, Ind. Eng. Chem. Res. 33 (1994) 548.
[57] J.M. Andresen, J.J. Strohm, L. Sun, C. Song, Energy Fuels 15 (2001) 714.
[58] J.J. Strohm, A.J. Brandt, S. Eser, C. Song, Prepr. Pap. - Am. Chem. Soc., Div. Fuel Chem. 48 (2003) 857.